
**Liquid Crystals**
Publication details, including instructions for authors and subscription information:
http://www.informaworld.com/smpp/title~content=t713926090

# Dynamics of surface anchoring breaking in a nematic liquid crystal

A. Gharbi[ab]; F. R. Fekih[a]; G. Durand[a]
[a] Laboratoire de Physique des Solides, Centre Universitaire, Orsay Cedex, France [b] Faculté des Sciences de Tunis, Department of Physics, Campus Universitaire, Tunis, Tunisia

**To cite this Article** Gharbi, A. , Fekih, F. R. and Durand, G.(1992) 'Dynamics of surface anchoring breaking in a nematic liquid crystal', Liquid Crystals, 12: 3, 515 — 520
**To link to this Article: DOI:** 10.1080/02678299208031064
**URL:** http://dx.doi.org/10.1080/02678299208031064

LIQUID CRYSTALS, 1992, VOL. 12, NO. 3, 515–520

# PRELIMINARY COMMUNICATIONS

## Dynamics of surface anchoring breaking in a nematic liquid crystal

by A. GHARBI†, F. R. FEKIH† and G. DURAND*
Laboratoire de Physique des Solides, Bâtiment 510,
Centre Universitaire, 91405 Orsay Cedex, France

(*Received 2 January 1992; accepted 26 April 1992*)

We present a simple dynamical model which describes the time dependence of the threshold electric field for breaking the surface anchoring of nematics. This model includes a surface friction, resulting from volume hydrodynamic dissipation. Experimental data with AC and DC pulsed fields are explained by this model. For DC, the threshold difference versus the field polarity is well-described by the flexoelectric effects in a uniform field for short times and in a non-uniform field for long times.



The surface anchoring of nematic liquid crystals has generally been studied in the static case. Recently dynamical measurements of the threshold voltage needed to break the nematic surface anchoring has been reported [1]. The experimental data show an increase of the threshold voltage when the duration of the applied electric field decreases. This behaviour seems to be a general property of the dynamics of the surface anchoring of nematics. In this preliminary communication we present a simple dynamical model which describes this time dependence of the threshold voltage by introducing a surface friction, resulting from volume hydrodynamic dissipation. To verify this model, new experiments have been performed.

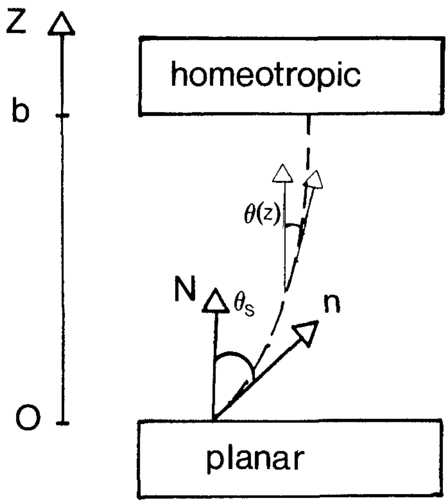


Figure 1. Hybrid cell geometry. The lower plate anchoring is represented as half broken with orientation $\theta_s$.

* Author for correspondence.
† On leave from Faculté des Sciences de Tunis, Department of Physics, Campus Universitaire, 1060 Tunis, Tunisia.

In [1] a nematic liquid crystal cell, doped with chiral ions was used. Each surface presents a bistable anchoring. To simplify the experiment, in the present work we use a nematic hybrid cell of thickness $d$ (see figure 1) where only one planar anchoring break occurs. To calculate the corresponding threshold voltage, we consider, as usual, the torque equation for the planar surface. Let us write this equation for both static and dynamic cases. We call $oz$ the axis perpendicular to the plates and $\theta(z)$ the assumed small angle which the nematic director makes with this axis. $\theta_s$ is the average value of $\theta$ on the planar anchoring, when an electric field is applied perpendicular to the plates. We use a nematic with a dielectric anisotropy $\varepsilon_a > 0$. The equilibrium volume torque density for small angles is [2]

$$\frac{\varepsilon_a E^2}{4\pi}\theta + K\frac{\partial^2\theta}{\partial z^2} + \eta\frac{\partial\theta}{\partial t} = 0, \tag{1}$$

here $K \approx K_3$ is the curvature constant and $\eta$ is the average viscosity of the nematic, taking into account backflow effects. In principle to calculate the breaking anchoring threshold field, we must integrate equation (1) over the volume.

In the static case $(\eta(\partial\theta/\partial t) = 0)$, the volume integrated dielectric torque induces a surface torque which can be written as

$$\Gamma_d = \int_1^2 \frac{\varepsilon_a E^2}{4\pi}\theta(z)\,dz = -\int_1^2 K\frac{\partial^2\theta}{\partial z^2}dz = +K\frac{\partial\theta_s}{\partial z}; \tag{2}$$

the limits 1 and 2 indicate respectively the planar and the homeotropic surfaces. By using the relation between $\theta(z)$ and $\theta_s$[2], for small angles, $\theta(z) = \theta_s \exp(-z/\xi_E)$, where $\xi_E = (1/|E|)(4\pi K/\varepsilon_a)^{1/2}$ is the coherence length, we can deduce

$$\frac{\partial\theta_s}{\partial z} = \frac{\sin\theta_s}{\xi_E}; \tag{3}$$

then

$$\Gamma_d = \frac{K}{\xi_E}\sin\theta_s. \tag{4}$$

For a nematic with $\varepsilon_a > 0$, $\Gamma_d$ tends to align the director toward $oz$. It is balanced by the surface elastic torque $\Gamma_s$, which has the usual Rapini–Papoular form [3],

$$\Gamma_s = -\frac{K}{L}\frac{\sin 2\theta_s}{2}$$

where $L$ is the extrapolation length. The minus sign indicates that the energy minimum is planar anchoring. The equation for the equilibrium torque for small angles is then

$$\frac{K}{\xi_E}\theta_s - \frac{K}{L}\theta_s = 0. \tag{5}$$

To break the anchoring, means to find a solution of equation (5) for $\theta_s \neq 0$; this gives

$$\frac{K}{\xi_E} - \frac{K}{L} = 0, \text{ i.e. } \xi_E = L$$

The static threshold field is then

$$|E_s| = \frac{1}{L}\left(\frac{4\pi K}{\varepsilon_a}\right)^{1/2}. \tag{6}$$

For the dynamic threshold, we start again from the volume torques in equation (1). We now have in addition the friction torque density: $\eta\partial\theta/\partial t$. Here also, the torque transmitted from the bulk to the surface is always $K\ \partial\theta_s/\partial z$. But now, $\theta$ depends on $z$ and $t$, and we cannot, in principle, separate a dielectric torque and a viscous torque. It is not the scope of this work to present an exact solution. If we assume now that $\theta(z, t)$ factorizes as $f(z)g(t)$, we can conserve the existence of independent dielectric and viscous torques. $f(z)$ is expected to vary only with the coherence length $\xi_E$. The dielectric torque has the same expression $(K/\xi_E)\theta_s$, and we have just to introduce a new surface friction torque

$$\Gamma_\eta = -\xi_E\eta\frac{\theta_s}{\tau}. \tag{7}$$

In the surface breaking limit ($\theta_s \approx 0$), the equation for the surface torque becomes

$$\frac{K}{\xi_E}\theta_s - \frac{K}{L}\theta_s - \xi_E\frac{\eta}{\tau}\theta_s = 0 \tag{8}$$

From this equation, we deduce the dynamic threshold field $E_{th}(\tau)$ to be

$$E_{th}(E_{th} - E_s) = \frac{4\pi}{\varepsilon_a}\frac{\eta}{\tau}. \tag{9}$$

As expected, $E_{th}(\tau)$ increases when $\tau$ decreases and for large values of $\tau$, tends towards the static threshold $E_s$.

To verify this model quantitatively we have performed an experiment with a hybrid nematic cell: one plate was silane coated for homeotropic alignment and the other SiO evaporated for planar alignment [4]. The cell has a fixed thickness $d$ of 2·2 $\mu$m and was filled with 4-$n$-pentyl-4′-cyanobiphenyl (5CB), which has $\varepsilon_a = 13{\cdot}5$ at 24°C [5]. To break the anchoring we have used, first, an AC field with a frequency (40 kHz) high enough to eliminate ionic effects. To observe the dynamic of the breaking we have used for the applied AC field an envelope of a square wave shape of duration $\tau$. The signal is zero between the AC burst pulses. Figure 2 shows the curve which corresponds to the rms threshold field $E_{th}(\tau)$. As expected, $E_{th}(\tau)$ decreases when $\tau$ increases.

The experimental data given in figure 2, have been compared to the calculation. By fitting to equation (9), we can deduce that $E_s^{AC} = 8{\cdot}5$ V $\mu$m$^{-1}$ and $\eta^{AC} = 29$ P. $E_s^{AC}$ which is the static threshold value, is in good agreement with the experimental measurements in [1]. However $\eta$ is two orders of magnitude larger than the average viscosity of 5CB ($\eta = 0{\cdot}5$ P). If we believe in our simplified dynamic model, this could indicate the existence of other causes of dissipation, such as a variation in the surface order parameter of the nematic when breaking the surface.

On the other hand, we have also measured the threshold field by using DC fields with two opposite polarities. The experimental data, given in figure 3, show two different curves $E_{th}^+(\tau)$ and $E_{th}^-(\tau)$ which decrease when $\tau$ increases. The average curve $(1/2)(E_{th}^- + E_{th}^+)$, can also be fitted by equation (9) with $E_s^{DC} = 7{\cdot}5$ V $\mu$m$^{-1}$ and $\eta^{DC} = 8$ P. $E_s^{DC}$ is comparable to $E_s^{AC}$. We do not understand clearly the difference in the AC and DC experimental values of $\eta$. This could be due to an effect of ions which intervenes differently in these measurements. We observe also that even for the DC case, $\eta$ is an order of magnitude higher than that for 5CB.

In the following, we show that we can also explain the $E_{th}^+$ and $E_{th}^-$ difference, with an improved model. We introduce the flexo-electric effect, supposed to arise only from a

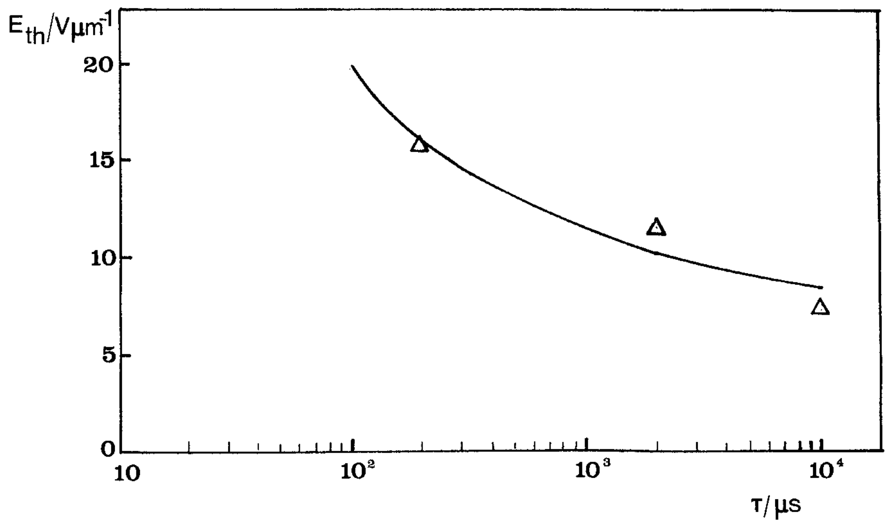


Figure 2. Threshold electric field $E_{th}$ versus the time duration $\tau$ of $E$ for 5CB at 25°C: triangles are the AC experimental data ($\nu = 40$ kHz); full line is the calculated curve from equation (9).



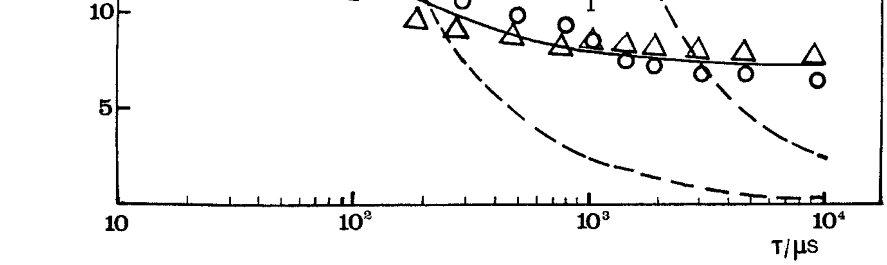


Figure 3. Threshold electric fields $E_{th}^{\pm}$ versus time duration $\tau$ for 5CB at 24°C: circles and triangles are the experimental data for $E_{th}^{+}$ and $E_{th}^{-}$ respectively, full line is the calculated $E_{th}$ from equation (9) for an averaged value (1/2) $(E_{th}^{+} + E_{th}^{-})$; dashed lines correspond to $E_{\mu}$ for $\mu_1 = 10^{-5}$ cm V$^{-1}$ s$^{-1}$ and $\mu_2 = 10^{-6}$ cm V$^{-1}$ s$^{-1}$.

quadrupolar origin. We first, assume that the electric field is uniform in the cell. The splay-bend distortion in a hybrid nematic cell induces a flexo-electric polarization [6]

$$P_f = -\nabla Q,$$

where $Q$ is the quadrupolar momentum. When an external electric field is applied across the plates, the free energy per unit area due to the flexopolarization is

$$F_1 = \int_1^2 -(PE)\,dz = \int_1^2 (\nabla Q)E\,dz = \int_1^2 eE\sin\theta\cos\theta\,d\theta; \tag{10}$$

it integrates out as a surface term. This gives the flexo-electric surface torque as

$$\Gamma_f = -(1/2)e\sin 2\theta_s E$$

and for small angles

$$\Gamma_f^{\pm} = +e\theta_s|E|; \tag{11}$$

$e = e_1 + e_3$ is the sum of the splay and bend flexo-electric coefficients. Introducing expression (11) into the torque equation (5), we can deduce by a simple calculation for $E_{th}^{\pm}$, the following expression

$$E_{th}^{\pm}\left[E_{th}^{\pm}\left(1+e\left(\frac{4\pi}{\varepsilon_a K}\right)^{1/2}\right)-E_s\right]=\frac{4\pi}{\varepsilon_a}\frac{\eta}{\tau}. \tag{12}$$

There is now, a difference between $E_{th}^{+}$ and $E_{th}^{-}$. From equation (12) and for 5CB where $e > 0$, we expect that for every $\tau$, $E_{th}^{+}$ is larger than $E_{th}^{-}$. Figure 3 does show this effect for small $\tau$ ($\tau < 1$ ms). From the experimental data, we have calculated the flexo-electric coefficient $e$, by using the expression

$$e=\left[\frac{(E_{th}^{+})^2-(E_{th}^{-})^2-E_s(E_{th}^{+}-E_{th}^{-})}{(E_{th}^{+})^2+(E_{th}^{-})^2}\right]\left(\frac{\varepsilon_a K}{4\pi}\right)^{1/2}. \tag{13}$$

deduced from equation (12). For $\tau = 60\,\mu$s, $E_{th}^{+} = 16{\cdot}5\ \mathrm{V}\,\mu\mathrm{m}^{-1}$ and $E_{th}^{-} = 14\ \mathrm{V}\,\mu\mathrm{m}^{-1}$, we deduce $e = 4{\cdot}1 \times 10^{12}\,\mathrm{C\,m}^{-1}$. This value is lower than the expected bulk value $21 \times 10^{-12}\,\mathrm{C\,m}^{-1}$, but compares with a recent measurement on an SiO rough surface [7].

Now, what happens for $\tau > 1$ ms? An idea to describe the threshold inversion between $E_{th}^{+}$ and $E_{th}^{-}$ for $\tau > 1$ ms, is to introduce ionic effects. For the large electric fields used, an ionic current appears as a motion of charges bouncing back and forth [8] between the two electrodes. We introduce now the transit time $\tau_t = d/\mu E$ of the ions; $\mu$ is the ion (common) mobility. For 5CB, $\mu$ ranges from $10^{-6}$–$10^{-5}\,\mathrm{cm\,V^{-1}\,s^{-1}}$ [8]. In figure 3 we have plotted in dashed lines the curves $E\mu = d/\mu\tau_t$ for $\mu = 10^{-5}$ and $10^{-6}\,\mathrm{cm\,V^{-1}\,s^{-1}}$. The inversion point I on the $E_{th}^{+}$ and $E_{th}^{-}$ curves is placed between the two curves $E_\mu$ and it separates into two regions:

(i) $\tau < 1$ ms, the ions do not have time to move. The field is uniform as previously discussed with the normal flexo-electric effect;

(ii) $\tau > 1$ ms, the ions have time to move inducing a non-uniform charge density and a non-uniform field: close to the plates, the electric field $E$ on the surface is larger than in the centre of the cell.

We discuss now, the polar effect of the field gradient. We consider the nematic in a non-uniform field. The free energy per unit area can be written as:

$$F_2 = \int -Q(\nabla E)dz. \tag{14}$$

To simplify, we assume that when the field gradient appears, the nematic ordering does not change significantly, i.e. $Q$ is uniform. From the identity:

$$\nabla(QE) = Q(\nabla E) + (\nabla Q)E \tag{15}$$

we find now $F_2 = -F_1$. The flexo-electric effect for the non-uniform electric field from hetero charges, has the opposite sign to the uniform electric case. This can explain the observed inversion of $E_{th}^{\pm}$ for $\tau > 1$ ms.

In conclusion, we have presented experimental data on the dynamics of field induced surface anchoring breaking in a nematic liquid crystal. A simplified model including a surface friction of pure hydrodynamic origin leads to an expected threshold increase when working with short pulses. This model explains qualitatively the experimental behaviour for AC and DC pulses. The order of magnitude of the effective viscosity is however too large, suggesting the introduction of other causes of dissipation. In DC, the threshold difference versus the field polarity is well-described by the flexo-electric effects in a uniform field for small $\tau$, and a non-uniform field gradient for large times, where ions have time to build counter charges close to the electrodes.

This work was supported by a French–Tunisian CNRS-FNRST exchange program.

## References

[1] Barberi, R., and Durand, G., 1991, *Appl. Phys. Lett.*, **58,** 2907.
[2] de Gennes, P. G., 1974, *The Physics of Liquid Crystals* (Clarendon Press).
[3] Rapini, A., and Papoular, M., 1969, *J. Phys., Paris Colloque*, **30,** C4–54.
[4] Monkade, M., Boix, M., and Durand, G., 1988, *Europhysics Lett.*, **5,** 697.
[5] Bradshaw, M. J., Raynes, E. P., Bunning, J. D., and Faber, T. E., 1985, *J. Phys., Paris*, **46,** 1513.
[6] Meyer, J. B., 1969, *Phys. Rev. Lett.*, **22,** 918.
[7] Blinov, L., and Durand, G. 1992, *J. Phys., Paris* (to be published).
[8] Vaxiviere, J., Labroo, B., and Martinot-Lagarde, Ph., 1989, *Molec. Crystals liq. Crystals*, **173,** 61.